FLORE
Repository istituzionale dell'Università degli Studi di Firenze

Tensor--product surface patches with Pythagorean--hodograph isoparametric curves

Tensor-product surface patches with Pythagorean-hodograph isoparametric curves

Rida T. Farouki

Department of Mechanical and Aerospace Engineering,
University of California, Davis, CA 95616, USA.

Francesca Pelosi

Dipartimento di Matematica, Università di Roma "Tor Vergata,"
Via della Ricerca Scientifica, 00133 Roma, Italy.

Maria Lucia Sampoli

Dipartimento di Ingegneria dell'Informazione e
Scienze Matematiche, Università di Siena, San Niccolò,
Via Roma 56, 53100 Siena, Italy.

Alessandra Sestini

Dipartimento di Matematica e Informatica, Università di Firenze,
Viale Morgagni 67/A, 50134 Firenze, Italy.

Abstract

The construction of tensor–product surface patches with a family of Pythagorean–hodograph (PH) isoparametric curves is investigated. The simplest non–trivial instances, interpolating four prescribed patch boundary curves, involve degree $(5,4)$ tensor–product surface patches $\mathbf{x}(u,v)$ whose $v = $ constant isoparametric curves are all spatial PH quintics. It is shown that the construction can be reduced to solving a novel type of quadratic quaternion equation, in which the quaternion unknown and its conjugate exhibit left and right coefficients, while the quadratic term has a coefficient interposed between them. A closed–form solution for this type of equation is derived, and conditions for

the existence of solutions are identified. The surfaces incorporate three residual scalar freedoms which can be exploited to improve the interior shape of the patch. The implementation of the method is illustrated through a selection of computed examples.

e–mail: farouki@ucdavis.edu, pelosi@mat.uniroma2.it,
marialucia.sampoli@unisi.it, alessandra.sestini@unifi.it

1 Introduction

The most commonly–used surface form in computer–aided geometric design is the tensor–product surface patch $\mathbf{x}(u, v)$ defined by a vector mapping from the unit parameter square $(u, v) \in [\,0, 1\,] \times [\,0, 1\,]$ to $\mathbb{R}^3$. A typical construct involves determining a smooth surface from four prescribed boundary curves $\mathbf{x}(u, 0), \mathbf{x}(u, 1), \mathbf{x}(0, v), \mathbf{x}(1, v)$ through a "transfinite interpolation" scheme — a problem first solved by the well–known *Coons patch* [5, 22].

The parameterization of a surface is a necessary artifact in specifying and analyzing its geometry. Although the isoparametric curves $u = \text{constant}$ and $v = \text{constant}$ have no intrinsic geometrical significance, they are nevertheless useful in practical applications, such as path planning for the machining or inspection of surfaces. In the simplest cases, where $\mathbf{x}(u, v)$ is a *ruled surface* or *bilinear surface*, its dependence on one or both of the parameters is linear, so the corresponding isoparametric curves are straight lines, and the parameters represent *distance* along the isoparametric curves. For higher–order surfaces, however, the parameters have no obvious geometrical meaning.

It is impossible to parameterize any curve, other than a straight line, by "simple" functions of its arc length [19, 20]. Nevertheless, the *Pythagorean–hodograph* (PH) *curves* have a distinct advantage over "ordinary" polynomial curves in this respect, since their arc lengths are simply *polynomial* functions of the curve parameter [9]. Many algorithms for the construction of planar and spatial PH curves have been developed, e.g., [13, 17, 24, 25, 27, 30, 35, 37]. The intent of the present paper is to investigate the feasibility of constructing surface patches with *Pythagorean–hodograph isoparametric curves*. The ruled and bilinear (doubly–ruled) surfaces are the simplest cases of such surfaces, but their generalization to higher–order surfaces is a non–trivial problem — especially under the constraint of prescribed boundary conditions.

Two different algebraic models are used in the construction of PH curves: the *complex number* representation [6] for planar PH curves, and quaternion representation [4, 11] for spatial PH curves. Since the isoparametric curves of a surface are (in general) space curves, the quaternion form is employed in the present study — this form is *rotation–invariant* [11], and subsumes the complex–number form as a special instance. Apart from its practical value in geometric design applications, the construction of surfaces with isoparametric PH curves leads naturally to the study of the solutions to certain algebraic equations in quaternion variables, with quaternion coefficients.

The focus of the present study is on surfaces that have a single family of

isoparametric PH curves, emphasizing specifically the Coons construction of defining such surfaces that interpolate four prescribed boundary curves. In particular, a closed–from solution is developed for the construction of a degree $(5, 4)$ tensor–product patch $\mathbf{x}(u, v)$ in which $\mathbf{x}(u, 0)$, $\mathbf{x}(u, 1)$ are prescribed PH quintics; $\mathbf{x}(0, v)$, $\mathbf{x}(1, v)$ are prescribed quartics; and for each fixed $v \in (0, 1)$ the curves $\mathbf{x}(u, v)$ are all PH quintics. The construction yields three residual free parameters, which can be used to manipulate the interior patch shape.

The plan for the remainder of this paper is as follows. First, some facts concerning the quaternion representation for spatial PH curves, and its use in defining surfaces with isoparametric PH curves, are reviewed in Section 2. The advantageous computational properties of such surfaces are then briefly summarized in Section 3. The simplest non–trivial instance of the problem is addressed in Section 4 — namely, the construction of a degree $(5, 4)$ surface patch $\mathbf{x}(u, v)$ with given boundary curves, whose $v = $ constant isoparametric curves are all PH quintics. This problem entails solving a pair of simultaneous linear quaternion equations, and a quadratic equation in a single quaternion variable and its conjugate, that has left, right, and intermediate quaternion coefficients dependent upon three free parameters. The closed–form solutions to these equations are developed in Section 5, and strategies to select the free parameters, so as to improve the interior surface shape, are briefly discussed in Section 6. Some computed examples, illustrating the solution procedure and the types of surface that can be constructed, are presented in Section 7. Finally, Section 8 summarizes the principal results of the present study, and identifies directions for further profitable investigation.

2   Surfaces with isoparametric PH curves

A PH curve $\mathbf{r}(u)$ is characterized by the property that its parametric speed $\sigma(u) = |\mathbf{r}'(u)|$ is a polynomial in the curve parameter u. The trivial instance $\sigma(u) = $ constant defines a straight line. Thus, as noted in Section 1, ruled and bilinear surfaces trivially have isoparametric PH curves. Moreover, since the only quadratic PH curves are degree–elevated straight lines, any biquadratic surface with isoparametric PH curves is a degree–elevated bilinear surface. The simplest non–trivial spatial PH curves are cubics, but to secure sufficient design flexibility the PH quintics are generally preferred.

A spatial PH curve $\mathbf{r}(u)$ is generated from a quaternion[1] polynomial $\mathcal{A}(u)$

---

[1]Calligraphic characters such as $\mathcal{A}$ denote quaternions, which are regarded as consisting

by integrating the form

$$\mathbf{r}'(u) \;=\; \mathcal{A}(u)\,\mathbf{i}\,\mathcal{A}^*(u)\,, \tag{1}$$

with $\mathcal{A}^*(u)$ being the conjugate of $\mathcal{A}(u)$. At present, we confine our attention to surfaces having a single family of isoparametric PH curves. Requiring *both* families of isoparametric curves to be PH curves incurs a more severe set of constraints, so the likelihood of obtaining non–trivial low–degree solutions, interpolating prescribed boundary curves, is therefore much lower.

One method of generalizing (1), so as to define a surface $\mathbf{x}(u,v)$ with PH curves as the $v = $ constant isoparametric loci, is to set

$$\mathbf{x}_u(u,v) \;=\; f(v)\,\mathcal{A}(u)\,\mathbf{i}\,\mathcal{A}^*(u) \tag{2}$$

for some scalar polynomial $f(v)$. Integration with respect to u yields a surface $\mathbf{x}(u,v)$ of odd degree in u, but the degree in v is equal to that of $f(v)$, which may be freely chosen. However, this formulation is quite restrictive: it implies that, along the $u = $ constant isoparametric curves, the surface derivative $\mathbf{x}_u$ in the u–direction can vary in magnitude but not in direction — consequently, these curves are all straight lines, and (2) defines a ruled surface.

To obtain a more flexible formulation, a bivariate quaternion polynomial $\mathcal{A}(u,v)$ must be used to defined $\mathbf{x}(u,v)$. Consider a tensor–product surface $\mathbf{x}(u,v)$ defined on $(u,v) \in [\,0,1\,] \times [\,0,1\,]$ whose $v = $ constant isoparametric curves are all PH curves, constructed from the expression

$$\mathbf{x}_u(u,v) \;=\; \mathcal{A}(u,v)\,\mathbf{i}\,\mathcal{A}^*(u,v)\,, \tag{3}$$

where we write the bivariate quaternion polynomial $\mathcal{A}(u,v)$ in terms of the Bernstein basis functions

$$b_k^d(t) \;=\; \binom{d}{k}(1-t)^{d-k}t^k\,, \quad k = 0,\ldots,d$$

in the form

$$\mathcal{A}(u,v) \;=\; \sum_{i=0}^{m}\sum_{j=0}^{n} \mathcal{A}_{ij}\,b_i^m(u)b_j^n(v)\,. \tag{4}$$

---

of a scalar part a and vector part $\mathbf{a}$, so that $\mathcal{A} = (a,\mathbf{a})$ and $a = \mathrm{scal}(\mathcal{A})$, $\mathbf{a} = \mathrm{vect}(\mathcal{A})$. See Chapter 5 of [9] for a review of the quaternion algebra pertinent to the present context.

Integrating with respect to u gives

$$\mathbf{x}(u,v) = \mathbf{r}(v) + \int \mathbf{x}_u(u,v)\,\mathrm{d}u\,,$$

the isoparametric curve $\mathbf{r}(v) = \mathbf{x}(0,v)$ being freely chosen. We assume it to be of degree $2n$, written in the form

$$\mathbf{r}(v) = \sum_{j=0}^{2n} \mathbf{p}_{0j}\, b_j^{2n}(v)\,. \tag{5}$$

Using the product rule [18] for Bernstein–form polynomials, the expression (3) becomes

$$\mathcal{A}(u,v)\,\mathbf{i}\,\mathcal{A}^*(u,v) = \sum_{i=0}^{2m}\sum_{j=0}^{2n} \mathbf{a}_{ij}\, b_i^{2m}(u)\, b_j^{2n}(v)\,, \tag{6}$$

where[2]

$$\mathbf{a}_{ij} = \sum_{k=\max(0,i-m)}^{\min(m,i)}\sum_{l=\max(0,j-n)}^{\min(n,j)} \frac{\binom{m}{k}\binom{m}{i-k}}{\binom{2m}{i}}\frac{\binom{n}{l}\binom{n}{j-l}}{\binom{2n}{j}}\, \mathcal{A}_{kl}\,\mathbf{i}\,\mathcal{A}^*_{i-k,j-l} \tag{7}$$

for $i = 0,\ldots,2m$ and $j = 0,\ldots,2n$. Hence, by the integration rule [18] for Bernstein–form polynomials, we obtain

$$\mathbf{x}(u,v) = \sum_{i=0}^{2m+1}\sum_{j=0}^{2n} \mathbf{p}_{ij}\, b_i^{2m+1}(u)\, b_j^{2n}(v)\,, \tag{8}$$

where the control points $\mathbf{p}_{0j}$ for $j = 0,\ldots,2n$ are freely chosen, and the remaining control points are specified by

$$\mathbf{p}_{ij} = \mathbf{p}_{i-1,j} + \frac{1}{2m+1}\,\mathbf{a}_{i-1,j} \tag{9}$$

for $i = 1,\ldots,2m+1$ and $j = 0,\ldots,2n$. Note that the surface (8) is of odd degree in u and even degree in v. If equal degrees in u and v are desired, one can impose a unit degree elevation on v.

---

[2]Note that the product (3) generates a pure vector expression.

3   Properties of isoparametric PH curves

For each fixed $v \in [0, 1]$ the parametric speed of the isoparametric PH curves is defined by

$$\sigma(u, v) \;=\; |\mathbf{x}_u(u, v)| \;=\; |\mathcal{A}(u, v)|^2 \;=\; \frac{\mathrm{d}s}{\mathrm{d}u}, \tag{10}$$

where s is arc length along a curve $\mathbf{x}(u, v)$ with $v = $ constant. Since $|\mathcal{A}(u, v)|^2 = \mathcal{A}(u, v)\,\mathcal{A}^*(u, v)$, from (4) we obtain

$$\sigma(u, v) \;=\; \sum_{i=0}^{2m} \sum_{j=0}^{2n} \sigma_{ij}\, b_i^{2m}(u)\, b_j^{2n}(v), \tag{11}$$

where

$$\sigma_{ij} \;=\; \sum_{k=\max(0, i-m)}^{\min(m,i)} \;\sum_{l=\max(0, j-n)}^{\min(n,j)} \frac{\binom{m}{k}\binom{m}{i-k}}{\binom{2m}{i}} \frac{\binom{n}{l}\binom{n}{j-l}}{\binom{2n}{j}} \, \mathcal{A}_{kl}\, \mathcal{A}^*_{i-k, j-l} \tag{12}$$

for $i = 0, \ldots, 2m$ and $j = 0, \ldots, 2n$. Hence, any $v = $ constant isoparametric curve has total arc length

$$S(v) \;=\; \frac{1}{2m+1} \sum_{j=0}^{2n} \left(\sum_{i=0}^{2m} \sigma_{ij} \right) b_j^{2n}(v). \tag{13}$$

The fact that the parametric speed of a PH curve is a polynomial in the curve parameter is especially advantageous in digital motion control. When a fabrication or inspection tool is to be driven along a surface isoparametric curve at a prescribed (constant or variable) speed $V = \mathrm{d}s/\mathrm{d}t$, it is necessary to compute the parameter values u_k of the commanded positions (reference points) along the path at each time $t_k = k\Delta t$, for a digital controller with sampling interval Δt. The desired values u_k satisfy the equation

$$\int_0^{u_k} \frac{\sigma}{V} \, \mathrm{d}u \;=\; k\Delta t.$$

The fact that σ is a polynomial in u facilitates closed–form reduction of the integral on the left, not only for constant speed V, but also for various useful dependencies of time, arc length, curvature, etc. [15, 16, 21]. This facilitates the development of efficient and versatile *real–time interpolator* algorithms for multi–axis computer numerical control (CNC) machines.

Five–axis CNC machines, for example, employ two rotary axes to control the tool orientation, in addition to the three translational axes that control its position. For a ball–end (spherical) tool, the cutter location (CL) point is related to the cutter contact (CC) point through a displacement equal to the tool radius, in the surface normal direction. Traditionally, toolpaths and feedrates for surface machining have been computed offline, and specified in terms of CL points. However, surfaces with isoparametric PH curves can be directly machined from the analytic surface definition, the tool feedrate being specified directly in terms of the CC points, with the CL points computed from the exact surface normal. This can result in significant improvements in controlling the accuracy and smoothness of machined surfaces [31].

The bending energy of each $v = $ constant isoparametric curve — i.e., the integral of the squared curvature with respect to arc length — also admits a closed–form reduction. In the present context, this can be expressed as

$$E(v) \;=\; \int_0^1 \kappa^2(u, v)\,\sigma(u, v)\,\mathrm{d}u\,,$$

with $\kappa(u, v) = |\mathbf{x}_u(u, v) \times \mathbf{x}_{uu}(u, v)|/\sigma^3(u, v)$. The method is described in the context of planar PH curves in [7], but readily extends to spatial PH curves. For each v, one must compute the complex–conjugate root pairs u of $\sigma(u, v)$ in order to perform a partial–fraction decomposition of the integrand.

For each v, the isoparametric PH quintic curve $\mathbf{x}(u, v)$ is equipped with a rational "adapted" orthonormal frame $(\mathbf{e}_1(u, v), \mathbf{e}_2(u, v), \mathbf{e}_3(u, v))$ defined by

$$(\mathbf{e}_1, \mathbf{e}_2, \mathbf{e}_3) \;=\; \frac{(\mathcal{A}\,\mathbf{i}\,\mathcal{A}, \mathcal{A}\,\mathbf{j}\,\mathcal{A}, \mathcal{A}\,\mathbf{k}\,\mathcal{A})}{|\mathcal{A}|^2}\,,$$

and known [3] as the *Euler–Rodrigues frame* (ERF). Here $\mathbf{e}_1$ is the tangent to the isoparametric PH curve, while $\mathbf{e}_2, \mathbf{e}_3$ span its normal plane. It is possible [10, 14] to construct spatial PH curves that have *rational rotation–minimizing frames* $(\mathbf{t}, \mathbf{u}, \mathbf{v})$ — known as *RRMF curves* — for which $\mathbf{t} = \mathbf{e}_1$ is again the tangent, but the normal–plane vectors $\mathbf{u}, \mathbf{v}$ exhibit no instantaneous rotation about $\mathbf{t}$, i.e., the frame angular velocity $\boldsymbol{\omega}$ satisfies $\boldsymbol{\omega} \cdot \mathbf{t} \equiv 0$. Such curves are of interest in robotics, computer animation, and swept surface constructions.

The *Darboux frame* $(\mathbf{n}, \mathbf{t}, \mathbf{h})$ along a surface curve is specified [29] by the surface normal $\mathbf{n}$, curve tangent $\mathbf{t}$, and tangent normal $\mathbf{h} = \mathbf{n} \times \mathbf{t}$. A *line of curvature* on a surface is tangent to a principal direction of curvature at each point. It can also be characterized by the property that the Darboux frame

6

is rotation–minimizing with respect to the curve tangent along it. Hence, if the boundary curves $\mathbf{x}(u,0)$ and $\mathbf{x}(u,1)$ are RRMF quintics, and the surface is constructed such that its normal $\mathbf{n}$ coincides with $\mathbf{u}$ or $\mathbf{v}$ (or any constant vector relative to them), these boundary curves will be lines of curvature [1].

More generally, it is possible to determine the rotation–minimizing frame orientation along any spatial PH quintic in closed form [8] — even if it is not an RRMF curve. This fact can be useful in specifying the attitude of a tool or probe that follows an isoparametric PH curve on a surface.

4   Construction of degree $(5,4)$ patches

Consider the problem of fixing the boundary curves of the patch (8). The boundary $\mathbf{x}(0,v)$ is just the curve (5) arising in the integration of (3), with freely–chosen control points $\mathbf{p}_{0j}$ for $j = 0, \ldots, 2n$. From equations (7)–(9), the boundary curves $\mathbf{x}(u,0)$ and $\mathbf{x}(u,1)$ can be expressed in the form

$$\mathbf{x}(u,0) \;=\; \sum_{i=0}^{2m+1} \mathbf{p}_{i0}\, b_i^{2m+1}(u)\,, \quad \mathbf{x}(u,1) \;=\; \sum_{i=0}^{2m+1} \mathbf{p}_{i,2n}\, b_i^{2m+1}(u)\,,$$

with control points $\mathbf{p}_{00}, \ldots, \mathbf{p}_{2m+1,0}$ and $\mathbf{p}_{0,2n}, \ldots, \mathbf{p}_{2m+1,2n}$ that depend only on the coefficients $\mathcal{A}_{00}, \ldots, \mathcal{A}_{m0}$ and $\mathcal{A}_{0n}, \ldots, \mathcal{A}_{mn}$ respectively, which can be used to freely design the boundary curves $\mathbf{x}(u,0)$ and $\mathbf{x}(u,1)$ by, for example, interpolation of first–order Hermite data with spatial PH quintics [13]. The boundary curve $\mathbf{x}(1,v)$ then remains to be determined.

The case $m = n = 1$ is the simplest non–trivial instance of (6), in which the $u = $ constant isoparametric curves are quadratic — i.e., planar parabola segments, while the $v = $ constant curves are spatial PH cubics. The boundary curve $\mathbf{x}(0,v)$ can be prescribed as a parabola segment through freely–chosen control points $\mathbf{p}_{00}, \mathbf{p}_{01}, \mathbf{p}_{02}$. If the coefficients $\mathcal{A}_{00}, \mathcal{A}_{10}$ and $\mathcal{A}_{01}, \mathcal{A}_{11}$ are then used to specify the boundary curves $\mathbf{x}(u,0)$ and $\mathbf{x}(u,1)$ as spatial PH cubics, there are no remaining freedoms, and the boundary curve $\mathbf{x}(1,v)$ will be a pre–determined parabola segment. Since this case is evidently too restrictive for most design applications, we do not further pursue it here.

We focus henceforth on the case $m = n = 2$ of (6) — which determines, on integrating (3), a surface patch $\mathbf{x}(u,v)$ whose $v = $ constant isoparametric curves are spatial PH quintics, and whose $u = $ constant isoparametric curves are "ordinary" quartics. It is shown below that, in this case, all four boundary curves can be prescribed so as to permit a Coons–type patch construction.

The boundary curve $\mathbf{x}(0, v)$ can be freely specified as a quartic by control points $\mathbf{p}_{00}, \mathbf{p}_{01}, \mathbf{p}_{02}, \mathbf{p}_{03}, \mathbf{p}_{04}$. If the coefficients $\mathcal{A}_{00}, \mathcal{A}_{10}, \mathcal{A}_{20}$ and $\mathcal{A}_{02}, \mathcal{A}_{12}, \mathcal{A}_{22}$ are used to construct the boundary curves $\mathbf{x}(u, 0)$ and $\mathbf{x}(u, 1)$ as first–order spatial PH quintic Hermite interpolants [13], then $\mathcal{A}_{01}, \mathcal{A}_{11}, \mathcal{A}_{21}$ remain as free coefficients. Of the five control points $\mathbf{p}_{50}, \mathbf{p}_{51}, \mathbf{p}_{52}, \mathbf{p}_{53}, \mathbf{p}_{54}$ specifying the remaining boundary curve $\mathbf{x}(1, v)$, the patch corner points $\mathbf{p}_{50}$ and $\mathbf{p}_{54}$ have already been determined in fixing $\mathbf{x}(u, 0)$ and $\mathbf{x}(u, 1)$. It is shown below that the remaining free quaternions $\mathcal{A}_{01}, \mathcal{A}_{11}, \mathcal{A}_{21}$ can be used to impart assigned positions to the control points $\mathbf{p}_{51}, \mathbf{p}_{52}, \mathbf{p}_{53}$ in closed form.

Let $\mathcal{A}_{00}, \mathcal{A}_{10}, \mathcal{A}_{20}$ and $\mathcal{A}_{02}, \mathcal{A}_{12}, \mathcal{A}_{22}$ be pre–determined by specifying the boundaries $\mathbf{x}(u, 0)$ and $\mathbf{x}(u, 1)$ as interpolants to the first–order Hermite data

$$\mathbf{x}(0, 0) = \mathbf{p}_{00}\,, \quad \mathbf{x}_u(0, 0) \qquad \text{and} \qquad \mathbf{x}(1, 0) = \mathbf{p}_{50}\,, \quad \mathbf{x}_u(1, 0)$$

and

$$\mathbf{x}(0, 1) = \mathbf{p}_{04}\,, \quad \mathbf{x}_u(0, 1) \qquad \text{and} \qquad \mathbf{x}(1, 1) = \mathbf{p}_{54}\,, \quad \mathbf{x}_u(1, 1)$$

respectively, through the algorithms in [13]. The dependence of the remaining three control points $\mathbf{p}_{51}, \mathbf{p}_{52}, \mathbf{p}_{53}$ on the free coefficients $\mathcal{A}_{01}, \mathcal{A}_{11}, \mathcal{A}_{21}$ can be determined from cases $j = 1, 2, 3$ of (9).

The expressions for the vectors $\mathbf{a}_{i1}, \mathbf{a}_{i2}, \mathbf{a}_{i3}$ are rather involved, and can be found in the Appendix. On substituting these expressions into (9), and noting that $\mathrm{vect}(\mathcal{U}\,\mathbf{i}\,\mathcal{V}^*) = \mathrm{vect}(\mathcal{V}\,\mathbf{i}\,\mathcal{U}^*)$ for any given quaternions $\mathcal{U}$ and $\mathcal{V}$, the coefficients $\mathcal{A}_{01}, \mathcal{A}_{11}, \mathcal{A}_{21}$ must satisfy the system of equations

$$\mathrm{vect}(\tilde{\mathcal{A}}_{00}\,\mathbf{i}\,\mathcal{A}_{01}^* + \tilde{\mathcal{A}}_{10}\,\mathbf{i}\,\mathcal{A}_{11}^* + \tilde{\mathcal{A}}_{20}\,\mathbf{i}\,\mathcal{A}_{21}^*) \;=\; 30\,(\mathbf{p}_{51} - \mathbf{p}_{01})\,, \qquad (14)$$

$$\begin{aligned} 12\,\mathcal{A}_{01}\,\mathbf{i}\,\mathcal{A}_{01}^* &+ 8\,\mathcal{A}_{11}\,\mathbf{i}\,\mathcal{A}_{11}^* + 12\,\mathcal{A}_{21}\,\mathbf{i}\,\mathcal{A}_{21}^* \\ &+ \mathrm{vect}(12\,\mathcal{A}_{01}\,\mathbf{i}\,\mathcal{A}_{11}^* + 4\,\mathcal{A}_{01}\,\mathbf{i}\,\mathcal{A}_{21}^* + 12\,\mathcal{A}_{11}\,\mathbf{i}\,\mathcal{A}_{21}^*) \\ &= 90\,(\mathbf{p}_{52} - \mathbf{p}_{02}) - \mathrm{vect}(\mathcal{W})\,, \end{aligned} \qquad (15)$$

$$\mathrm{vect}(\tilde{\mathcal{A}}_{02}\,\mathbf{i}\,\mathcal{A}_{01}^* + \tilde{\mathcal{A}}_{12}\,\mathbf{i}\,\mathcal{A}_{11}^* + \tilde{\mathcal{A}}_{22}\,\mathbf{i}\,\mathcal{A}_{21}^*) \;=\; 30\,(\mathbf{p}_{53} - \mathbf{p}_{03})\,, \qquad (16)$$

where

$$\begin{bmatrix} \tilde{\mathcal{A}}_{00} \\ \tilde{\mathcal{A}}_{10} \\ \tilde{\mathcal{A}}_{20} \end{bmatrix} = \begin{bmatrix} 6 & 3 & 1 \\ 3 & 4 & 3 \\ 1 & 3 & 6 \end{bmatrix} \begin{bmatrix} \mathcal{A}_{00} \\ \mathcal{A}_{10} \\ \mathcal{A}_{20} \end{bmatrix}, \quad \begin{bmatrix} \tilde{\mathcal{A}}_{02} \\ \tilde{\mathcal{A}}_{12} \\ \tilde{\mathcal{A}}_{22} \end{bmatrix} = \begin{bmatrix} 6 & 3 & 1 \\ 3 & 4 & 3 \\ 1 & 3 & 6 \end{bmatrix} \begin{bmatrix} \mathcal{A}_{02} \\ \mathcal{A}_{12} \\ \mathcal{A}_{22} \end{bmatrix}$$

and

$$\mathcal{W} \;=\; \tilde{\mathcal{A}}_{02}\,\mathbf{i}\,\mathcal{A}_{00}^{*} + \tilde{\mathcal{A}}_{12}\,\mathbf{i}\,\mathcal{A}_{10}^{*} + \tilde{\mathcal{A}}_{22}\,\mathbf{i}\,\mathcal{A}_{20}^{*} \;=\; \mathcal{A}_{02}\,\mathbf{i}\,\tilde{\mathcal{A}}_{00}^{*} + \mathcal{A}_{12}\,\mathbf{i}\,\tilde{\mathcal{A}}_{10}^{*} + \mathcal{A}_{22}\,\mathbf{i}\,\tilde{\mathcal{A}}_{20}^{*}$$

are known quaternions once $\mathcal{A}_{00}, \mathcal{A}_{10}, \mathcal{A}_{20}$ and $\mathcal{A}_{02}, \mathcal{A}_{12}, \mathcal{A}_{22}$ have been fixed in determining the boundary curves $\mathbf{x}(u,0)$ and $\mathbf{x}(u,1)$.

Let $\mathcal{B} = (b, \mathbf{b})$ and $\mathcal{C} = (c, \mathbf{c})$ have free scalar parts b and c, and vector parts $\mathbf{b} = 30\,(\mathbf{p}_{51} - \mathbf{p}_{01})$ and $\mathbf{c} = 30\,(\mathbf{p}_{53} - \mathbf{p}_{03})$. Then equations (14) and (16) can be written in the form

$$\tilde{\mathcal{A}}_{00}\,\mathbf{i}\,\mathcal{A}_{01}^{*} + \tilde{\mathcal{A}}_{20}\,\mathbf{i}\,\mathcal{A}_{21}^{*} \;=\; \mathcal{B} - \tilde{\mathcal{A}}_{10}\,\mathbf{i}\,\mathcal{A}_{11}^{*}\,,$$
$$\tilde{\mathcal{A}}_{02}\,\mathbf{i}\,\mathcal{A}_{01}^{*} + \tilde{\mathcal{A}}_{22}\,\mathbf{i}\,\mathcal{A}_{21}^{*} \;=\; \mathcal{C} - \tilde{\mathcal{A}}_{12}\,\mathbf{i}\,\mathcal{A}_{11}^{*}\,. \tag{17}$$

These simultaneous linear equations determine $\mathcal{A}_{01}^{*}$ and $\mathcal{A}_{21}^{*}$ in terms of $\mathcal{A}_{11}^{*}$ and the parameters b and c. Setting $\mathcal{M}_{11} = \tilde{\mathcal{A}}_{00}\,\mathbf{i}$, $\mathcal{M}_{12} = \tilde{\mathcal{A}}_{20}\,\mathbf{i}$, $\mathcal{M}_{21} = \tilde{\mathcal{A}}_{02}\,\mathbf{i}$, $\mathcal{M}_{22} = \tilde{\mathcal{A}}_{22}\,\mathbf{i}$, $\mathcal{Y}_{1} = \mathcal{B} - \tilde{\mathcal{A}}_{10}\,\mathbf{i}\,\mathcal{A}_{11}^{*}$, $\mathcal{Y}_{2} = \mathcal{C} - \tilde{\mathcal{A}}_{12}\,\mathbf{i}\,\mathcal{A}_{11}^{*}$, the equations can be solved by an adaptation of Gaussian elimination to the quaternion algebra, as described in Section 5.1. The solutions are of the form

$$\mathcal{A}_{01}^{*} \;=\; \mathcal{E}_{01} - \mathcal{F}_{01}\mathcal{A}_{11}^{*}\,, \quad \mathcal{A}_{21}^{*} \;=\; \mathcal{E}_{21} - \mathcal{F}_{21}\mathcal{A}_{11}^{*}\,, \tag{18}$$

where

$$\mathcal{E}_{01} \;=\; \mathcal{N}_{11}\mathcal{B} + \mathcal{N}_{12}\mathcal{C}\,, \quad \mathcal{F}_{01} \;=\; (\mathcal{N}_{11}\tilde{\mathcal{A}}_{10} + \mathcal{N}_{12}\tilde{\mathcal{A}}_{12})\,\mathbf{i}\,, \tag{19}$$
$$\mathcal{E}_{21} \;=\; \mathcal{N}_{21}\mathcal{B} + \mathcal{N}_{22}\mathcal{C}\,, \quad \mathcal{F}_{21} \;=\; (\mathcal{N}_{21}\tilde{\mathcal{A}}_{10} + \mathcal{N}_{22}\tilde{\mathcal{A}}_{12})\,\mathbf{i}\,, \tag{20}$$

and the known quantities $\mathcal{N}_{11}, \mathcal{N}_{12}, \mathcal{N}_{21}, \mathcal{N}_{22}$ are as given in Section 5.1.

If $\mathcal{D} = (d, \mathbf{d})$ has free scalar part d and vector part $\mathbf{d} = 90\,(\mathbf{p}_{52} - \mathbf{p}_{02}) - \mathrm{vect}(\mathcal{W})$, equation (15) can be written as

$$12\,\mathcal{A}_{01}\,\mathbf{i}\,\mathcal{A}_{01}^{*} + 8\,\mathcal{A}_{11}\,\mathbf{i}\,\mathcal{A}_{11}^{*} + 12\,\mathcal{A}_{21}\,\mathbf{i}\,\mathcal{A}_{21}^{*}$$
$$+\; 12\,\mathcal{A}_{01}\,\mathbf{i}\,\mathcal{A}_{11}^{*} + 4\,\mathcal{A}_{01}\,\mathbf{i}\,\mathcal{A}_{21}^{*} + 12\,\mathcal{A}_{11}\,\mathbf{i}\,\mathcal{A}_{21}^{*} \;=\; \mathcal{D}\,.$$

Substituting from (18), we obtain the quadratic equation

$$\mathcal{A}_{11}\,\mathcal{P}\,\mathcal{A}_{11}^{*} + \mathcal{A}_{11}\,\mathcal{Q} + \mathcal{R}\,\mathcal{A}_{11}^{*} \;=\; \mathcal{S}\,, \tag{21}$$

in $\mathcal{A}_{11}$, where the known quaternions $\mathcal{P}, \mathcal{Q}, \mathcal{R}, \mathcal{S}$ are defined by

$$\mathcal{P} \;=\; 12\,(\mathcal{F}_{01}^{*}\,\mathbf{i}\,\mathcal{F}_{01} + \mathcal{F}_{21}^{*}\,\mathbf{i}\,\mathcal{F}_{21}) + 4\,\mathcal{F}_{01}^{*}\,\mathbf{i}\,\mathcal{F}_{21} + 8\,\mathbf{i} - 12\,(\mathcal{F}_{01}^{*}\,\mathbf{i} + \mathbf{i}\,\mathcal{F}_{21})\,,$$
$$\mathcal{Q} \;=\; 12\,\mathbf{i}\,\mathcal{E}_{21} - 12\,(\mathcal{F}_{01}^{*}\,\mathbf{i}\,\mathcal{E}_{01} + \mathcal{F}_{21}^{*}\,\mathbf{i}\,\mathcal{E}_{21}) - 4\,\mathcal{F}_{01}^{*}\,\mathbf{i}\,\mathcal{E}_{21}\,,$$
$$\mathcal{R} \;=\; 12\,\mathcal{E}_{01}^{*}\,\mathbf{i} - 12\,(\mathcal{E}_{01}^{*}\,\mathbf{i}\,\mathcal{F}_{01} + \mathcal{E}_{21}^{*}\,\mathbf{i}\,\mathcal{F}_{21}) - 4\,\mathcal{E}_{01}^{*}\,\mathbf{i}\,\mathcal{F}_{21}\,,$$
$$\mathcal{S} \;=\; \mathcal{D} - 12\,(\mathcal{E}_{01}^{*}\,\mathbf{i}\,\mathcal{E}_{01} + \mathcal{E}_{21}^{*}\,\mathbf{i}\,\mathcal{E}_{21}) - 4\,\mathcal{E}_{01}^{*}\,\mathbf{i}\,\mathcal{E}_{21}\,. \tag{22}$$

Note that equation (21) contains three real parameters — $b = \mathrm{scal}(\mathcal{B})$ and $c = \mathrm{scal}(\mathcal{C})$, upon which $\mathcal{E}_{01}$ and $\mathcal{E}_{21}$ depend as in (19)–(20), and $d = \mathrm{scal}(\mathcal{D})$.

Thus, the construction of a surface $\mathbf{x}(u, v)$ with prescribed boundaries, whose $v = $ constant isoparametric curves are all spatial PH quintics, has been reduced to solving the quadratic equation (21) in the quaternion variable $\mathcal{A}_{11}$. This equation has a closed–form solution, as described in Section 5.2 below.

5   Analysis of the quaternion equations

Because of the non–commutative quaternion product, the problem of solving equations in quaternion variables, with quaternion coefficients, is much more subtle than in the case of real or complex numbers. In the most general case, incorporating arbitrary juxtapositions of the variable and coefficients, there is no "fundamental theorem of algebra," since equations with no solutions can easily be constructed. Consequently, most studies consider only polynomials in which all coefficients are to the left or right of the powers of the quaternion variable, e.g., [23, 26, 28, 32, 33, 36]. Even in this restricted setting, unusual features — such as the occurrence of "spherical roots" — may arise.

At present, we need to solve the simultaneous linear equations (17) in the quaternion unknowns $\mathcal{A}_{01}^{*}$ and $\mathcal{A}_{21}^{*}$, and the quadratic equation (21) — with left, right, and interposed coefficients — in the quaternion unknown $\mathcal{A}_{11}$. We show here that both these problems admit closed–form solutions.

5.1   Simultaneous linear quaternion equations

Consider a system of two linear equations in two quaternion variables, with quaternion coefficients:

$$\begin{bmatrix} \mathcal{M}_{11} & \mathcal{M}_{12} \\ \mathcal{M}_{21} & \mathcal{M}_{22} \end{bmatrix} \begin{bmatrix} \mathcal{X}_1 \\ \mathcal{X}_2 \end{bmatrix} = \begin{bmatrix} \mathcal{Y}_1 \\ \mathcal{Y}_2 \end{bmatrix}. \tag{23}$$

Although the usual Gaussian elimination process does not hold, the system still has (in general) a unique solution, which may be determined as follows. Multiplying the first and second equations by $\mathcal{M}_{12}^{*}$ and $\mathcal{M}_{22}^{*}$ gives

$$\mathcal{M}_{12}^{*}\mathcal{M}_{11}\mathcal{X}_1 + |\mathcal{M}_{12}|^2 \mathcal{X}_2 = \mathcal{M}_{12}^{*}\mathcal{Y}_1 \,,$$
$$\mathcal{M}_{22}^{*}\mathcal{M}_{21}\mathcal{X}_1 + |\mathcal{M}_{22}|^2 \mathcal{X}_2 = \mathcal{M}_{22}^{*}\mathcal{Y}_2 \,,$$

from which we infer that

$$\mathcal{X}_2 \;=\; \frac{\mathcal{M}_{12}^*(\mathcal{Y}_1 - \mathcal{M}_{11}\mathcal{X}_1)}{|\mathcal{M}_{12}|^2} \;=\; \frac{\mathcal{M}_{22}^*(\mathcal{Y}_2 - \mathcal{M}_{21}\mathcal{X}_1)}{|\mathcal{M}_{22}|^2}\,.$$

For these two expression to be consistent, we must have

$$|\mathcal{M}_{22}|^2 \mathcal{M}_{12}^*(\mathcal{Y}_1 - \mathcal{M}_{11}\mathcal{X}_1) \;=\; |\mathcal{M}_{12}|^2 \mathcal{M}_{22}^*(\mathcal{Y}_2 - \mathcal{M}_{21}\mathcal{X}_1)\,,$$

or

$$\left(|\mathcal{M}_{12}|^2 \mathcal{M}_{22}^* \mathcal{M}_{21} - |\mathcal{M}_{22}|^2 \mathcal{M}_{12}^* \mathcal{M}_{11}\right)\mathcal{X}_1 \;=\; |\mathcal{M}_{12}|^2 \mathcal{M}_{22}^* \mathcal{Y}_2 - |\mathcal{M}_{22}|^2 \mathcal{M}_{12}^* \mathcal{Y}_1\,.$$

By analogous arguments, we can also infer that

$$\left(|\mathcal{M}_{11}|^2 \mathcal{M}_{21}^* \mathcal{M}_{22} - |\mathcal{M}_{21}|^2 \mathcal{M}_{11}^* \mathcal{M}_{12}\right)\mathcal{X}_2 \;=\; |\mathcal{M}_{11}|^2 \mathcal{M}_{21}^* \mathcal{Y}_2 - |\mathcal{M}_{21}|^2 \mathcal{M}_{11}^* \mathcal{Y}_1\,.$$

Multiplying both sides of these equations on the left by the inverses of the coefficients of $\mathcal{X}_1$ and $\mathcal{X}_2$, and simplifying, then gives the solution

$$\mathcal{X}_1 \;=\; \mathcal{N}_{11}\mathcal{Y}_1 + \mathcal{N}_{12}\mathcal{Y}_2\,, \quad \mathcal{X}_2 \;=\; \mathcal{N}_{21}\mathcal{Y}_1 + \mathcal{N}_{22}\mathcal{Y}_2\,,$$

where we set

$$\mathcal{N}_{11} \;=\; \frac{|\mathcal{M}_{22}|^2 \mathcal{M}_{11}^* - \mathcal{M}_{21}^* \mathcal{M}_{22} \mathcal{M}_{12}^*}{\Delta}\,, \quad \mathcal{N}_{12} \;=\; \frac{|\mathcal{M}_{12}|^2 \mathcal{M}_{21}^* - \mathcal{M}_{11}^* \mathcal{M}_{12} \mathcal{M}_{22}^*}{\Delta}\,,$$

$$\mathcal{N}_{21} \;=\; \frac{|\mathcal{M}_{21}|^2 \mathcal{M}_{12}^* - \mathcal{M}_{22}^* \mathcal{M}_{21} \mathcal{M}_{11}^*}{\Delta}\,, \quad \mathcal{N}_{22} \;=\; \frac{|\mathcal{M}_{11}|^2 \mathcal{M}_{22}^* - \mathcal{M}_{12}^* \mathcal{M}_{11} \mathcal{M}_{21}^*}{\Delta}\,.$$

with

$$\Delta \;=\; |\mathcal{M}_{11}|^2 |\mathcal{M}_{22}|^2 + |\mathcal{M}_{12}|^2 |\mathcal{M}_{21}|^2 - 2\,\mathrm{scal}(\mathcal{M}_{21}^* \mathcal{M}_{22} \mathcal{M}_{12}^* \mathcal{M}_{11})\,.$$

Note that $\Delta \geq |\mathcal{M}_{11}|^2 |\mathcal{M}_{22}|^2 + |\mathcal{M}_{12}|^2 |\mathcal{M}_{21}|^2 - 2\,|\mathcal{M}_{11}|\,|\mathcal{M}_{12}|\,|\mathcal{M}_{21}|\,|\mathcal{M}_{22}| = (|\mathcal{M}_{11}|\,|\mathcal{M}_{22}| - |\mathcal{M}_{12}|\,|\mathcal{M}_{21}|)^2 \geq 0$. The form

$$\begin{bmatrix} \mathcal{N}_{11} & \mathcal{N}_{12} \\ \mathcal{N}_{21} & \mathcal{N}_{22} \end{bmatrix}$$

can be considered the (left) inverse of the quaternion coefficient matrix in (23). The quantity $\sqrt{\Delta}$ is known [2] as the *Dieudonné determinant* of the matrix, and we must have $\Delta \neq 0$ for a unique solution to (23).

5.2 Quadratic quaternion equation

The form (21) is an unusual quaternion equation, in that the linear terms depend on both the variable and its conjugate, with coefficients on the left and right, and the coefficient of the quadratic term is inserted between them. By separating (21) into its $1, \mathbf{i}, \mathbf{j}, \mathbf{k}$ components, it can be regarded as a system of four quadratic equations in four real variables, the $1, \mathbf{i}, \mathbf{j}, \mathbf{k}$ components of $\mathcal{A}_{11}$. Numerical experiments show that this system can typically be solved by Newton–Raphson iteration, but this provides no indication whether a failure to converge is due to non–existence of solutions or to inappropriate starting approximations. Instead, we develop here an essentially closed–form solution procedure for equation (21) that offers greater insight into the conditions on the coefficients $\mathcal{P}, \mathcal{Q}, \mathcal{R}, \mathcal{S}$ ensuring the existence of solutions.

For brevity, we write the unknown $\mathcal{A}_{11}$ in (21) as $\mathcal{A} = (a, \mathbf{a})$. Similarly, let p, q, r, s and $\mathbf{p}, \mathbf{q}, \mathbf{r}, \mathbf{s}$ be the scalar and vector parts of $\mathcal{P}, \mathcal{Q}, \mathcal{R}, \mathcal{S}$. The cases $p = 0$ or $\mathbf{p} = \mathbf{0}$ identify degenerate cases of equation (21) that require separate treatment — see [12] for a detailed analysis. To avoid long technical diversions, we focus here on the generic case in which $p \neq 0$ and $\mathbf{p} \neq \mathbf{0}$. Now the scalar and vector parts of equation (21) can be written as

$$p\,(a^2 + |\mathbf{a}|^2) - (\mathbf{q} - \mathbf{r}) \cdot \mathbf{a} + (q + r)\,a \;=\; s\,, \tag{24}$$

$$2\,\mathcal{A}\,\mathbf{p}\,\mathcal{A}^* + \mathcal{A}\,\mathcal{Q} - \mathcal{Q}^*\mathcal{A}^* + \mathcal{R}\,\mathcal{A}^* - \mathcal{A}\,\mathcal{R}^* \;=\; 2\,\mathbf{s}\,. \tag{25}$$

Assuming that $p \neq 0$, equation (24) identifies $\mathcal{A}$ as lying on a 3–sphere in $\mathbb{R}^4$ with center and radius defined by

$$\mathcal{C} \;=\; -\,\frac{\mathcal{Q}^* + \mathcal{R}}{2\,p} \qquad \text{and} \qquad \rho \;=\; \frac{\sqrt{|\mathcal{Q}^* + \mathcal{R}|^2 + 4\,ps}}{2\,|p|}$$

provided that

$$|\mathcal{Q}^* + \mathcal{R}|^2 + 4\,ps \;\geq\; 0\,, \tag{26}$$

since (24) is then equivalent to $|\,\mathcal{A} - \mathcal{C}\,|^2 = \rho^2$. However, if condition (26) does not hold, equation (21) has no solution. Assuming that (26) holds, and introducing the unit quaternion

$$\mathcal{U} \;=\; \frac{\mathcal{A} - \mathcal{C}}{\rho}\,. \tag{27}$$

equation (21) can be re–formulated as

$$\mathcal{U}\,\mathcal{P}\,\mathcal{U}^* + \mathcal{U}\,\tilde{\mathcal{Q}} + \tilde{\mathcal{R}}\,\mathcal{U}^* \;=\; \tilde{\mathcal{S}}\,, \tag{28}$$

12

where we define the known quaternions

$$\tilde{\mathcal{Q}} = \frac{2\,p\,\mathcal{Q} - \mathcal{P}(\mathcal{Q} + \mathcal{R}^*)}{2\,\rho\,p}, \quad \tilde{\mathcal{R}} = \frac{2\,p\,\mathcal{R} - (\mathcal{Q}^* + \mathcal{R})\mathcal{P}}{2\,\rho\,p},$$

$$\tilde{\mathcal{S}} = \frac{1}{\rho^2}\left[\mathcal{S} + \frac{|\mathcal{Q}|^2 + |\mathcal{R}|^2 + 2\,\mathcal{R}\,\mathcal{Q}}{2\,p} - \frac{(\mathcal{Q}^* + \mathcal{R})\,\mathcal{P}\,(\mathcal{Q} + \mathcal{R}^*)}{4\,p^2}\right].$$

Note that the scalar part of equation (28) is automatically satisfied, so we need only consider the vector part. Now since $\mathcal{P} + \mathcal{P}^* = 2\,p$, one can verify that $\tilde{\mathcal{R}} = -\,\tilde{\mathcal{Q}}^*$, and equation (28) can be written as

$$\mathcal{U}\,\mathcal{P}\,\mathcal{U}^* + \mathcal{U}\,\tilde{\mathcal{Q}} - \tilde{\mathcal{Q}}^*\mathcal{U}^* = \tilde{\mathcal{S}}. \tag{29}$$

Furthermore, since $\mathcal{U}\,\tilde{\mathcal{Q}} - \tilde{\mathcal{Q}}^*\mathcal{U}^*$ is a pure vector, writing $\tilde{\mathcal{S}} = (\tilde{s}, \tilde{\mathbf{s}})$ the vector part of equation (29) becomes

$$\mathcal{U}\,\mathbf{p}\,\mathcal{U}^* + \mathcal{U}\,\tilde{\mathcal{Q}} - \tilde{\mathcal{Q}}^*\mathcal{U}^* = \tilde{\mathbf{s}}.$$

Setting

$$\mathcal{Z} = \mathcal{U} + \frac{\tilde{\mathcal{Q}}^*\,\mathbf{p}}{|\mathbf{p}|^2} \quad \text{and} \quad \mathbf{v} = \tilde{\mathbf{s}} + \frac{\tilde{\mathcal{Q}}^*\,\mathbf{p}\,\tilde{\mathcal{Q}}}{|\mathbf{p}|^2}, \tag{30}$$

this can be further reduced to obtain the equation

$$\mathcal{Z}\,\mathbf{p}\,\mathcal{Z}^* = \mathbf{v}. \tag{31}$$

If $\hat{\mathbf{p}} = \mathbf{p}/|\mathbf{p}|$ and $\hat{\mathbf{v}} = \mathbf{v}/|\mathbf{v}|$ are unit vectors in the direction of the known vectors $\mathbf{p}$ and $\mathbf{v}$, the general solution of (31) has [13] the form

$$\mathcal{Z} = \mathbf{z}\,\exp(\phi\,\hat{\mathbf{p}}), \quad \mathbf{z} = \sqrt{\frac{|\mathbf{v}|}{|\mathbf{p}|}}\,\frac{\hat{\mathbf{p}} + \hat{\mathbf{v}}}{|\hat{\mathbf{p}} + \hat{\mathbf{v}}|}, \tag{32}$$

where $\exp(\phi\,\hat{\mathbf{p}}) = \cos\phi + \sin\phi\,\hat{\mathbf{p}}$, the parameter $\phi \in [0, 2\pi)$ being chosen to ensure that

$$|\mathcal{U}|^2 = \left|\mathcal{Z} - \frac{\tilde{\mathcal{Q}}^*\,\mathbf{p}}{|\mathbf{p}|^2}\right|^2 = |\mathcal{Z}|^2 + 2\,\frac{\text{scal}(\mathcal{Z}\,\mathbf{p}\,\tilde{\mathcal{Q}})}{|\mathbf{p}|^2} + \frac{|\tilde{\mathcal{Q}}|^2}{|\mathbf{p}|^2} = 1. \tag{33}$$

Substituting from (32), this condition can be expanded to obtain

$$\alpha\,\sin\phi + \beta\,\cos\phi = \gamma, \tag{34}$$

13

where

$$\alpha = \frac{\hat{\mathbf{p}} + \hat{\mathbf{v}}}{|\,\hat{\mathbf{p}} + \hat{\mathbf{v}}\,|} \cdot \tilde{\mathbf{q}}, \quad \beta = \frac{(\hat{\mathbf{p}} \times \hat{\mathbf{v}}) \cdot \tilde{\mathbf{q}} - (1 + \hat{\mathbf{p}} \cdot \hat{\mathbf{v}})\,\tilde{q}}{|\,\hat{\mathbf{p}} + \hat{\mathbf{v}}\,|}, \quad \gamma = \frac{|\mathbf{p}|^2 - |\mathbf{p}|\,|\mathbf{v}| - |\tilde{\mathcal{Q}}|^2}{2\sqrt{|\mathbf{p}|\,|\mathbf{v}|}}.$$

Hence, defining ψ by the relations

$$\cos\psi = \frac{\alpha}{\sqrt{\alpha^2 + \beta^2}}, \quad \sin\psi = \frac{\beta}{\sqrt{\alpha^2 + \beta^2}},$$

we have

$$\sin(\phi + \psi) = \frac{\gamma}{\sqrt{\alpha^2 + \beta^2}}.$$

Thus, in addition to condition (26), the values α, β, γ must satisfy

$$|\gamma| \leq \sqrt{\alpha^2 + \beta^2} \tag{35}$$

in order for a solution to exist. When (35) is satisfied, equation (34) identifies, in general, two distinct ϕ values. For each value, a corresponding solution $\mathcal{A}$ ($= \mathcal{A}_{11}$) can be obtained from (27), (30), and (32).

Once equation (21) has been solved for $\mathcal{A}_{11}$, the corresponding $\mathcal{A}_{01}$ and $\mathcal{A}_{21}$ values are determined from (18) as

$$\mathcal{A}_{01} = \mathcal{E}_{01}^* - \mathcal{A}_{11}\mathcal{F}_{01}^*, \quad \mathcal{A}_{21} = \mathcal{E}_{21}^* - \mathcal{A}_{11}\mathcal{F}_{21}^*,$$

Knowing all the coefficients $\mathcal{A}_{ij}$ for $0 \leq i, j \leq 2$, the Bézier control points of the surface (8) can be computed from expressions (7) and (9).

6   Selection of free parameters

As observed in Section 4, the coefficients in equation (21) depend on the free scalar parameters $b = \mathrm{scal}(\mathcal{B})$, $c = \mathrm{scal}(\mathcal{C})$, $d = \mathrm{scal}(\mathcal{D})$ through expressions (19)–(20) and (22). Since the construction ensures precise matching of the prescribed patch boundary curves, these free parameters influence only the interior patch shape, and can be exploited to improve the shape. Because of the highly non–linear nature of equation (21), it is impractical to attempt to express the dependence of its solution, and of the geometrical properties of the resulting surface patch, on these free parameters.

14

However, by minimization of a suitable "shape functional," an automatic selection of the parameters can be achieved through a numerical optimization procdure. Shape optimization with respect to free parameters is a recurring theme in constrained–boundary surface constructions, and functionals based on higher–order shape measures (e.g., Guassian curvature or thin–plate spline energy) are often employed. Such measures can also be invoked in the present context, but since the main focus of this study is on formulating and solving the systems of quaternion equations described in Sections 4 and 5, for ease of computation we choose to minimize a simpler measure, namely, the mean arc length L of the $v = $ constant isoparametric PH curves. From expression (13) with $m = n = 2$, this measure can be expressed as

$$ L \; = \; \frac{1}{25} \sum_{i=0}^{4} \sum_{j=0}^{4} \sigma_{ij} \,. \tag{36} $$

Consistent with the prescribed patch boundary curves, this measure favors a "flatter" interior surface shape. Among the two possible solutions to (34) identified at each iteration of the optimization procedure, the one that yields the smaller L value is selected.

7 Computed examples

In each example, the quartic boundary curves $\mathbf{x}(0, v)$ and $\mathbf{x}(1, v)$ are defined by assigning their Bézier control points $\mathbf{p}_{0j}$ and $\mathbf{p}_{5j}$ for $j = 0, \ldots, 4$. The boundary curves $\mathbf{x}(u, 0)$ and $\mathbf{x}(u, 1)$ are constructed as PH quintic Hermite interpolants, using the CC criterion to fix the free angular parameters — see [13, 34]. The solution is then completely specified by assigning the corner u derivatives, $\mathbf{a}_{00} = \mathbf{x}_u(0, 0)$, $\mathbf{a}_{40} = \mathbf{x}_u(1, 0)$ and $\mathbf{a}_{04} = \mathbf{x}_u(0, 1)$, $\mathbf{a}_{44} = \mathbf{x}_u(1, 1)$. Also, since (22) implies that the parameter $d = \mathrm{scal}(\mathcal{D})$ is equivalent to a free choice for $s = \mathrm{scal}(\mathcal{S})$, the quantity s is always treated as a free parameter.

In the following examples, we report the results obtained by setting all the free parameters equal to zero, and by determining them through the use of an optimization procedure that minimizes the quantity (36). In fact we observe that, in the considered examples, setting the free parameters to zero always appears to produce a surface with "reasonable" shape.

The constructed surfaces are evaluated on a uniform 400×400 grid, with the isoparametric PH curves corresponding to $v = j/7$ for $j = 0, \ldots, 7$ shown
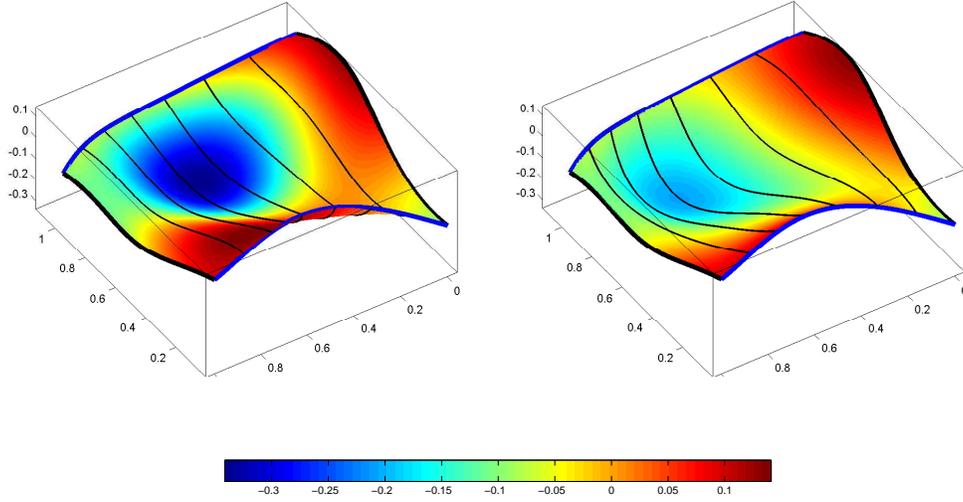
15

Figure 1: The two surface patches obtained in Example 1, when the values $b = c = s = 0$ are chosen for the free parameters. The corresponding values for the shape measure (36) are $L = 1.1136$ (left) and $L = 1.0616$ (right).

in black, while the assigned quartic boundary curves $\mathbf{x}(0, v)$ and $\mathbf{x}(1, v)$ are in blue. In some examples, in order to more clearly visualize the difference between the constructed surfaces, they are also shown color–coded according to the variation of the Gaussian curvature and mean curvature.

Example 1. In the first example the control points defining $\mathbf{x}(0, v)$ and $\mathbf{x}(1, v)$ are chosen as

$$
\begin{aligned}
\mathbf{p}_{00} &= (0, 0, -0.1), & \mathbf{p}_{50} &= (1, 0, 0.1), \\
\mathbf{p}_{01} &= (0.1, 0.2, 0), & \mathbf{p}_{51} &= (1.1, 0.3, 0), \\
\mathbf{p}_{02} &= (0.2, 0.5, 0.2), & \mathbf{p}_{52} &= (1.2, 0.6, -0.2), \\
\mathbf{p}_{03} &= (0.1, 0.7, 0.1), & \mathbf{p}_{53} &= (1.1, 0.8, 0), \\
\mathbf{p}_{04} &= (0, 1, 0.1), & \mathbf{p}_{54} &= (1, 1, -0.1),
\end{aligned}
$$

and the assigned corner derivatives

$$
\begin{aligned}
\mathbf{a}_{00} &= (0.9298, 0.2978, 0.2164), & \mathbf{a}_{40} &= (-0.8763, -0.4479, 0.1773), \\
\mathbf{a}_{04} &= (0.9686, 0.2312, -0.0915), & \mathbf{a}_{44} &= (-0.9298, -0.3226, -0.1773).
\end{aligned}
$$

For this example, when the free parameters b, c, s are set to zero, equation (34) admits two distinct solutions, corresponding to two different quaternion

16

solutions $\mathcal{A}_{11}$ of (21). The resulting surface patches are shown[3] in Figure 1. Figure 2 illustrates the surface obtained when the parameters are selected to minimize (36) using a numerical optimization procedure.
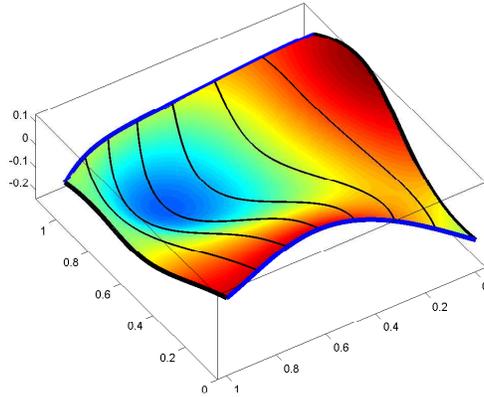

Figure 2: The surface obtained in Example 1 through minimization of (36) — the resulting values are $b = 0.3246$, $c = -0.4150$, $s = 0.0979$, and $L = 1.0588$.

Example 2. In the second example, the curves $\mathbf{x}(0, v)$ and $\mathbf{x}(1, v)$ are line segments, and hence the corresponding control points are collinear, namely

$$
\begin{aligned}
\mathbf{p}_{00} &= (1, 0, 0)\,, & \mathbf{p}_{50} &= (0.5, 0.866, 0.524)\,, \\
\mathbf{p}_{01} &= (1.125, 0.125, 0.910)\,, & \mathbf{p}_{51} &= (0.75, 1.116, 1.559)\,, \\
\mathbf{p}_{02} &= (1.25, 0.25, 1.82)\,, & \mathbf{p}_{52} &= (1.0, 1.366, 2.595)\,, \\
\mathbf{p}_{03} &= (1.375, 0.375, 2.731)\,, & \mathbf{p}_{53} &= (1.25, 1.616, 3.630)\,, \\
\mathbf{p}_{04} &= (1.5, 0.5, 3.642)\,, & \mathbf{p}_{54} &= (1.5, 1.866, 4.665)\,,
\end{aligned}
$$

while the corner derivatives are

$$
\begin{aligned}
\mathbf{a}_{00} &= (0, 1.0, 0.5)\,, & \mathbf{a}_{40} &= (-0.866, 0.5, 0.5)\,, \\
\mathbf{a}_{04} &= (0, 1.0, 0.5)\,, & \mathbf{a}_{44} &= (-0.866, 0.5, 0.5)\,.
\end{aligned}
$$

As in Example 1, setting all the free parameters to zero yields two different solutions, shown in Figure 3. In order to highlight the differences between the two surfaces, they are shown color–coded in Figure 4 according to the variation of their Gaussian curvature and mean curvature. The solution with

---

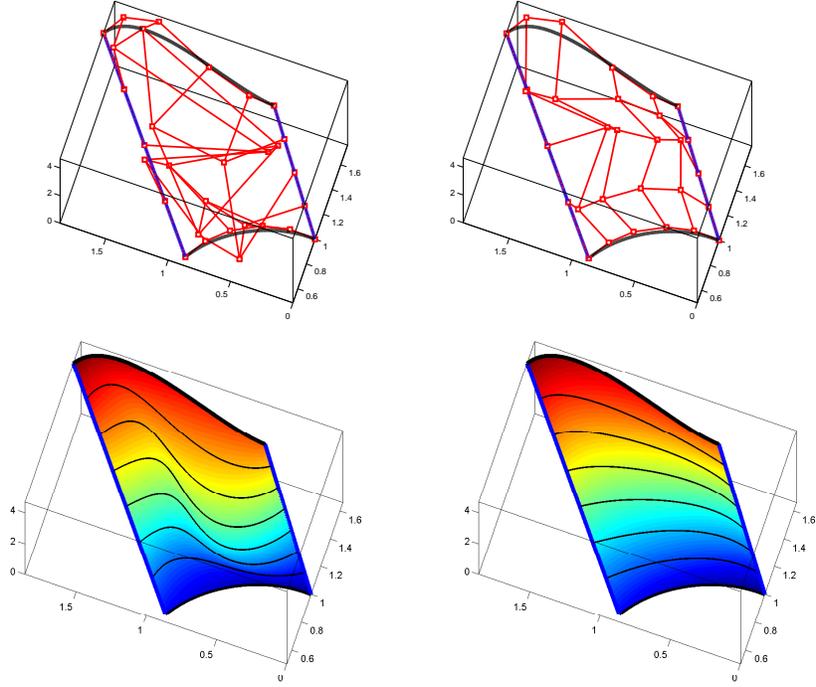[3]Unless otherwise noted, the color coding in the Figures indicates the surface z–height.

17

Figure 3: The surfaces obtained with $b = c = s = 0$ in Example 2. Upper: the given PH quintic curves $\mathbf{x}(u,0)$, $\mathbf{x}(u,1)$ (black) and the quartic polynomial curves $\mathbf{x}(0,v)$, $\mathbf{x}(1,v)$ (blue), together with the surface control net (red). Lower: the resulting surfaces with $L = 1.577$ (left) and $L = 1.415$ (right).

the smaller L value is clearly preferable. As is evident in Figure 5, a further improvement in surface quality is obtained by selecting the free parameters using the optimization procedure to minimize L.

Example 3. In the final example, the control points of the two boundary quartic curves are given by

$$\begin{array}{ll}
\mathbf{p}_{00} = (0,0,0)\,, & \mathbf{p}_{50} = (2,2,0)\,, \\
\mathbf{p}_{01} = (0,0,0.25)\,, & \mathbf{p}_{51} = (2,2,0.25)\,, \\
\mathbf{p}_{02} = (1.667,0,0.5)\,, & \mathbf{p}_{52} = (2,1.833,0.5)\,, \\
\mathbf{p}_{03} = (0.5,0,0.5)\,, & \mathbf{p}_{53} = (2,1.5,0.75)\,, \\
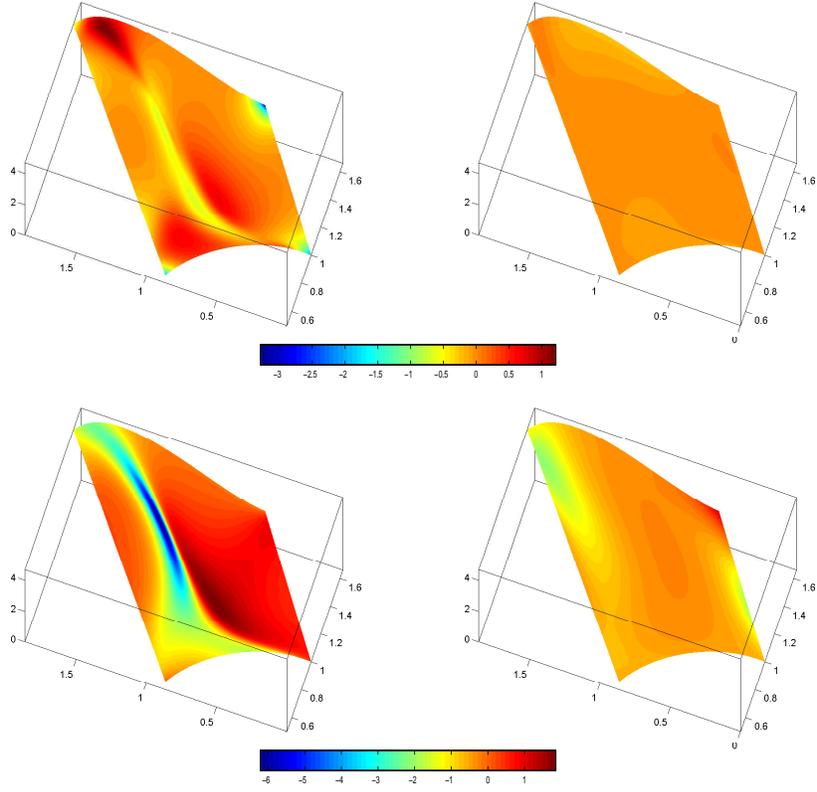\mathbf{p}_{04} = (1,0,1)\,, & \mathbf{p}_{54} = (2,1,1)\,,
\end{array}$$

Figure 4: The two surfaces obtained with the parameter values $b = c = s = 0$ in Example 2 are shown color–coded according to variation of their Gaussian curvature (upper) and mean curvature (lower).

and the corner derivatives are

$$\mathbf{a}_{00} = (0, 4, 0), \qquad \mathbf{a}_{40} = (4, 0, 0),$$
$$\mathbf{a}_{04} = (0, 1, 0), \qquad \mathbf{a}_{44} = (1, 0, 0).$$

In this example, equation (34) is an identity if the free parameters are zero since then $\alpha = \beta = \gamma = 0$, indicating that any ϕ in (32) ensures satisfaction of equation (33). In this case, $\mathcal{A}_{11}$ is chosen as close as possible to a weighted combination of the known quaternions $\mathcal{A}_{00}, \mathcal{A}_{10}, \mathcal{A}_{20}$ and $\mathcal{A}_{02}, \mathcal{A}_{12}, \mathcal{A}_{22}$, e.g., $\frac{1}{4}(\mathcal{A}_{00} + \mathcal{A}_{20} + \mathcal{A}_{02} + \mathcal{A}_{22})$. This solution, shown in Figure 6, proves to be the same as that produced by the minimization of L.
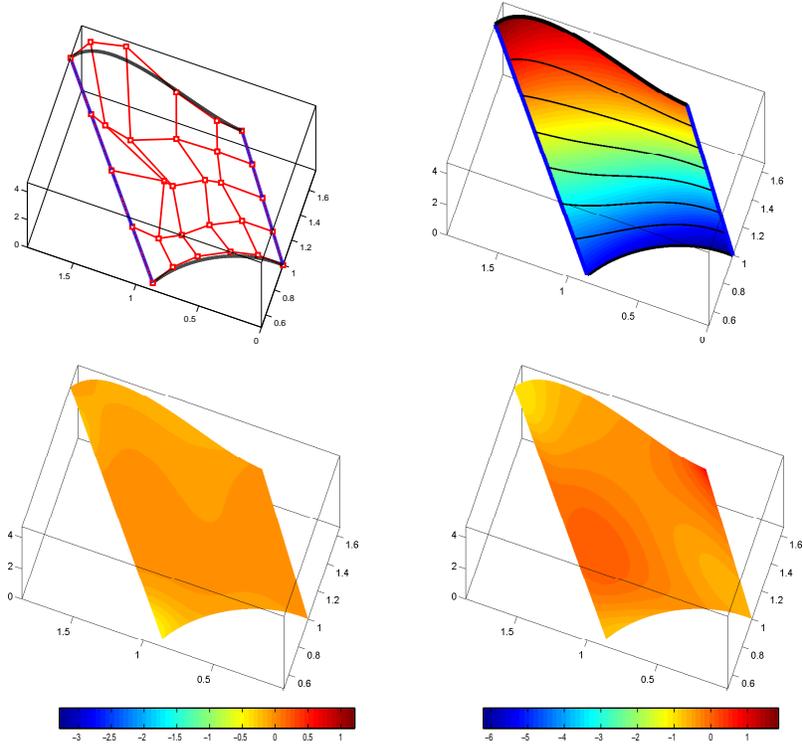
19

Figure 5: Example 2 with the optimized parameters $b = 7.4794$, $c = 11.4533$, $s = -1.4636$, giving $L = 1.3905$. Upper: the boundary curves together with the control net (left) and resulting surface (right). Lower: the surface color–coded using the Gaussian curvature (left) and mean curvature (right).

8 Closure

The construction of a tensor–product surface patch $\mathbf{x}(u, v)$ that incorporates a single family of isoparametric PH curves has been addressed in the simplest context allowing all four boundary curves to be prescribed, namely, a degree $(5, 4)$ patch whose $v = $ constant curves are spatial PH quintics. The problem is reduced to the solution of a special type of quadratic quaternion equation. A thorough analysis of this equation yields a closed–form solution procedure and conditions for the existence of solutions. For given boundary curves, the resulting surfaces depend on three scalar parameters, which can be exploited to adjust the interior shape of the surface patch. The implementation of the
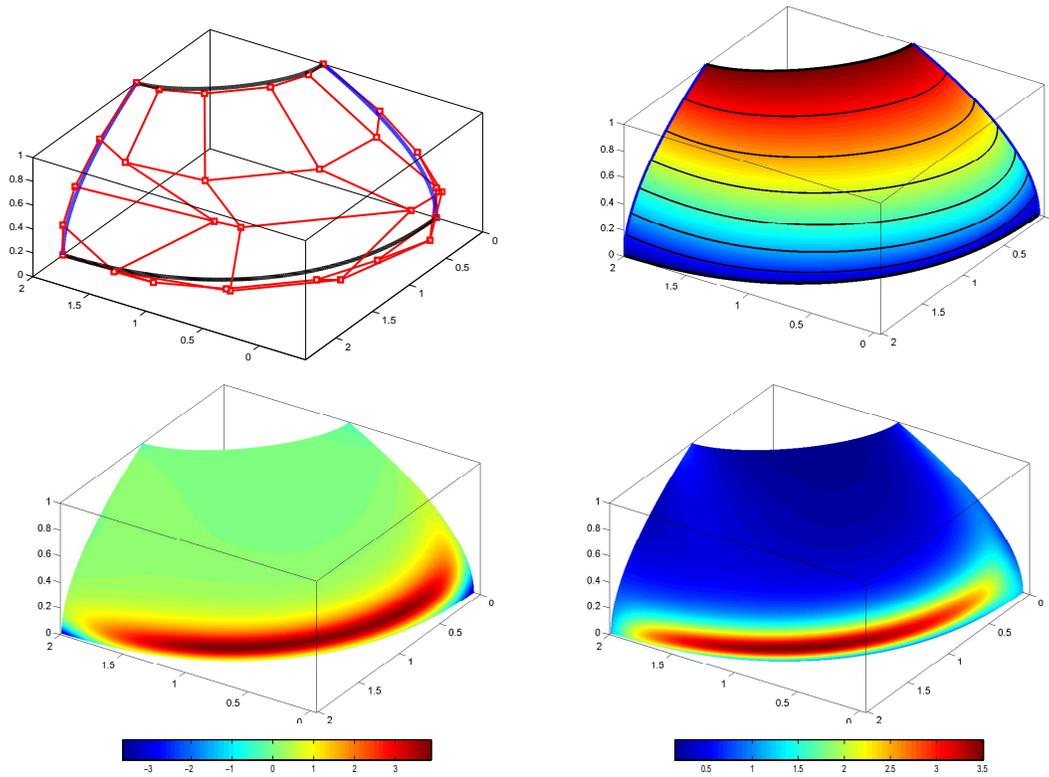
Figure 6: The surface obtained in Example 3 with $b = c = s = 0$, yielding the value $L = 2.9132$. Upper: the boundary curves together with the control net (left) and the resulting surface (right). Lower: the surface color–coded according to the Gaussian curvature (left) and mean curvature (right).

method is illustrated through a selection of computed examples.

Although preliminary and exploratory in nature, the present results are encouraging in that they elucidate an analytic solution procedure for a rather complicated non–linear problem. Nevertheless, many issues must be resolved in further developing this line of investigation — these include, for example, better insight into the geometrical significance of the free parameters, and if solutions are always possible through an appropriate choice for them; study of the surface shape quality compared with Coons patches constructed using "ordinary" polynomial curves; interpolating additional (e.g., surface normal) data along the prescribed boundary curves; and exploring the possibility of patches for which *both* sets of isoparametric loci are PH curves.

Appendix

The dependence of the three control points $\mathbf{p}_{51}, \mathbf{p}_{52}, \mathbf{p}_{53}$ on the free coefficients $\mathcal{A}_{01}, \mathcal{A}_{11}, \mathcal{A}_{21}$ is determined from cases $j = 1, 2, 3$ of (9). In particular, from (7) with $m = n = 2$ we have

$$\mathbf{a}_{i1} = \sum_{k=\max(0,i-2)}^{\min(2,i)} \sum_{l=0}^{1} \frac{\binom{2}{k}\binom{2}{i-k}}{\binom{4}{i}} \frac{\binom{2}{l}\binom{2}{1-l}}{\binom{4}{1}} \mathcal{A}_{kl} \, \mathbf{i} \, \mathcal{A}^*_{i-k,1-l} \,,$$

$$\mathbf{a}_{i2} = \sum_{k=\max(0,i-2)}^{\min(2,i)} \sum_{l=0}^{2} \frac{\binom{2}{k}\binom{2}{i-k}}{\binom{4}{i}} \frac{\binom{2}{l}\binom{2}{2-l}}{\binom{4}{2}} \mathcal{A}_{kl} \, \mathbf{i} \, \mathcal{A}^*_{i-k,2-l} \,,$$

$$\mathbf{a}_{i3} = \sum_{k=\max(0,i-2)}^{\min(2,i)} \sum_{l=1}^{2} \frac{\binom{2}{k}\binom{2}{i-k}}{\binom{4}{i}} \frac{\binom{2}{l}\binom{2}{3-l}}{\binom{4}{3}} \mathcal{A}_{kl} \, \mathbf{i} \, \mathcal{A}^*_{i-k,3-l} \,,$$

22

for $i = 0, \ldots, 4$. An explicit enumeration gives

$$
\begin{aligned}
\mathbf{a}_{01} &= \mathrm{vect}(\mathcal{A}_{00}\, \mathbf{i}\, \mathcal{A}_{01}^*)\,, \\
2\,\mathbf{a}_{11} &= \mathrm{vect}(\mathcal{A}_{00}\, \mathbf{i}\, \mathcal{A}_{11}^* + \mathcal{A}_{01}\, \mathbf{i}\, \mathcal{A}_{10}^*)\,, \\
6\,\mathbf{a}_{21} &= \mathrm{vect}(\mathcal{A}_{00}\, \mathbf{i}\, \mathcal{A}_{21}^* + \mathcal{A}_{01}\, \mathbf{i}\, \mathcal{A}_{20}^* + 4\,\mathcal{A}_{10}\, \mathbf{i}\, \mathcal{A}_{11}^*)\,, \\
2\,\mathbf{a}_{31} &= \mathrm{vect}(\mathcal{A}_{10}\, \mathbf{i}\, \mathcal{A}_{21}^* + \mathcal{A}_{11}\, \mathbf{i}\, \mathcal{A}_{20}^*) \\
\mathbf{a}_{41} &= \mathrm{vect}(\mathcal{A}_{20}\, \mathbf{i}\, \mathcal{A}_{21}^*)\,,
\end{aligned}
$$

$$
\begin{aligned}
3\,\mathbf{a}_{02} &= \mathrm{vect}(\mathcal{A}_{00}\, \mathbf{i}\, \mathcal{A}_{02}^*) + 2\,\mathcal{A}_{01}\, \mathbf{i}\, \mathcal{A}_{01}^*\,, \\
6\,\mathbf{a}_{12} &= \mathrm{vect}(\mathcal{A}_{00}\, \mathbf{i}\, \mathcal{A}_{12}^* + \mathcal{A}_{02}\, \mathbf{i}\, \mathcal{A}_{10}^* + 4\,\mathcal{A}_{01}\, \mathbf{i}\, \mathcal{A}_{11}^*)\,, \\
18\,\mathbf{a}_{22} &= \mathrm{vect}(\mathcal{A}_{00}\, \mathbf{i}\, \mathcal{A}_{22}^* + \mathcal{A}_{02}\, \mathbf{i}\, \mathcal{A}_{20}^* + 4\,\mathcal{A}_{01}\, \mathbf{i}\, \mathcal{A}_{21}^* + 4\,\mathcal{A}_{10}\, \mathbf{i}\, \mathcal{A}_{12}^*) + 8\,\mathcal{A}_{11}\, \mathbf{i}\, \mathcal{A}_{11}^*\,, \\
6\,\mathbf{a}_{32} &= \mathrm{vect}(\mathcal{A}_{10}\, \mathbf{i}\, \mathcal{A}_{22}^* + \mathcal{A}_{12}\, \mathbf{i}\, \mathcal{A}_{20}^* + 4\,\mathcal{A}_{11}\, \mathbf{i}\, \mathcal{A}_{21}^*)\,, \\
3\,\mathbf{a}_{42} &= \mathrm{vect}(\mathcal{A}_{20}\, \mathbf{i}\, \mathcal{A}_{22}^*) + 2\,\mathcal{A}_{21}\, \mathbf{i}\, \mathcal{A}_{21}^*\,,
\end{aligned}
$$

$$
\begin{aligned}
\mathbf{a}_{03} &= \mathrm{vect}(\mathcal{A}_{01}\, \mathbf{i}\, \mathcal{A}_{02}^*)\,, \\
2\,\mathbf{a}_{13} &= \mathrm{vect}(\mathcal{A}_{01}\, \mathbf{i}\, \mathcal{A}_{12}^* + \mathcal{A}_{02}\, \mathbf{i}\, \mathcal{A}_{11}^*) \\
6\,\mathbf{a}_{23} &= \mathrm{vect}(\mathcal{A}_{01}\, \mathbf{i}\, \mathcal{A}_{22}^* + \mathcal{A}_{02}\, \mathbf{i}\, \mathcal{A}_{21}^* + 4\,\mathcal{A}_{11}\, \mathbf{i}\, \mathcal{A}_{12}^*)\,, \\
2\,\mathbf{a}_{33} &= \mathrm{vect}(\mathcal{A}_{11}\, \mathbf{i}\, \mathcal{A}_{22}^* + \mathcal{A}_{12}\, \mathbf{i}\, \mathcal{A}_{21}^*) \\
\mathbf{a}_{43} &= \mathrm{vect}(\mathcal{A}_{21}\, \mathbf{i}\, \mathcal{A}_{22}^*)\,.
\end{aligned}
$$

Acknowledgements

References

[1] L. Biard, R. T. Farouki, and N. Szafran (2010), Construction of rational surface patches bounded by lines of curvature, *Comput. Aided Geom. Design* **27**, 359–371.

[2] C. Bisi and G. Gentili (2009), Möbius transformations and the Poincaré distance in the quaternionic setting, *Ind. Univ. J. Math.* **58**, 2729–2764.

[3] H. I. Choi and C. Y. Han (2002), Euler–Rodrigues frames on spatial Pythagorean–hodograph curves, *Comput. Aided Geom. Design* **19**, 603–620.

[4] H. I. Choi, D. S. Lee, and H. P. Moon (2002), Clifford algebra, spin representation, and rational parameterization of curves and surfaces, *Adv. Comp. Math.* **17**, 5–48.

[5] S. A. Coons (1967), Surfaces for computer aided design of space forms, Technical Report MAC–TR–41, MIT.

[6] R. T. Farouki (1994), The conformal map $z \to z^2$ of the hodograph plane, *Comput. Aided Geom. Design* **11**, 363–390.

[7] R. T. Farouki (1996), The elastic bending energy of Pythagorean–hodograph curves, *Comput. Aided Geom. Design* **13**, 227–241.

[8] R. T. Farouki (2002), Exact rotation–minimizing frames for spatial Pythagorean–hodograph curves, *Graph. Models* **64**, 382–395.

[9] R. T. Farouki (2008), *Pythagorean–Hodograph Curves: Algebra and Geometry Inseparable*, Springer, Berlin.

[10] R. T. Farouki (2010), Quaternion and Hopf map characterizations for the existence of rational rotation–minimizing frames on quintic space curves, *Adv. Comp. Math.* **33**, 331–348.

[11] R. T. Farouki, M. al–Kandari, and T. Sakkalis (2002), Structural invariance of spatial Pythagorean hodographs, *Comput. Aided Geom. Design* **19**, 395–407.

[12] R. T. Farouki, G. Gentili, C. Giannelli, A. Sestini, and C. Stoppato (2014), Solution of a class of quadratic quaternion equations, preprint.

[13] R. T. Farouki, C. Giannelli, C. Manni, and A. Sestini (2008), Identification of spatial PH quintic Hermite interpolants with

near–optimal shape measures, *Comput. Aided Geom. Design* **25**, 274–297.

[14] R. T. Farouki, C. Giannelli, C. Manni, and A. Sestini (2012), Design of rational rotation–minimizing rigid body motions by Hermite interpolation, *Math. Comp.* **81**, 879–903.

[15] R. T. Farouki, J. Manjunathaiah, D. Nicholas, G.–F. Yuan, and S. Jee (1998), Variable feedrate CNC interpolators for constant material removal rates along Pythagorean–hodograph curves, *Comput. Aided Design* **30**, 631–640.

[16] R. T. Farouki, J. Manjunathaiah, and G.–F. Yuan (1999), G codes for the specification of Pythagorean–hodograph tool paths and associated feedrate functions on open–architecture CNC machines, *Int. J. Mach. Tools Manuf.* **39**, 123–142.

[17] R. T. Farouki and C. A. Neff (1995), Hermite interpolation by Pythagorean–hodograph quintics, *Math. Comp.* **64**, 1589–1609.

[18] R. T. Farouki and V. T. Rajan (1988), Algorithms for polynomials in Bernstein form, *Comput. Aided Geom. Design* **5**, 1–26.

[19] R. T. Farouki and T. Sakkalis (1991), Real rational curves are not "unit speed," *Comput. Aided Geom. Design* **8**, 151–157.

[20] R. T. Farouki and T. Sakkalis (2007), Rational space curves are not "unit speed," *Comput. Aided Geom. Design* **24**, 238–240.

[21] R. T. Farouki and S. Shah (1996), Real–time CNC interpolators for Pythagorean–hodograph curves, *Comput. Aided Geom. Design* **13**, 583–600.

[22] A. R. Forrest (1972), On Coons' and other methods for the representation of curved surfaces, *Comput. Graphics Image Proc.* **1**, 341–359.

[23] G. Gentili and C. Stoppato (2008), Zeros of regular functions and polynomials of a quaternionic variable, *Mich. Math. J.* **56**, 655–667.

[24] C. Y. Han (2010), Geometric Hermite interpolation by monotone helical quintics, *Comput. Aided Geom. Design* **27**, 713–719.

[25] G. Jaklic, J. Kozak, M. Krajnc, V. Vitrih, and E. Zagar (2012), An approach to geometric interpolation by Pythagorean–hodograph curves, *Adv. Comp. Math.* **37**, 123–150.

[26] D. Janovská and G. Opfer (2010), A note on the computation of all zeros of simple quaternionic polynomials, *SIAM J. Numer. Anal.* **48**, 244–256.

[27] B. Jüttler (2001), Hermite interpolation by Pythagorean hodograph curves of degree seven, *Math. Comp.* **70**, 1089–1111.

[28] B. Kalantari (2013), Algorithms for quaternion polynomial root–finding, *J. Complexity* **29**, 302–322.

[29] E. Kreyszig (1959), *Differential Geometry*, University of Toronto Press.

[30] S. H. Kwon (2010), Solvability of G^1 Hermite interpolation by spatial Pythagorean–hodograph cubics and its selection scheme, *Comput. Aided Geom. Design* **27**, 138–149.

[31] K. M. Nittler and R. T. Farouki (2015), A real–time surface interpolator methodology for precision CNC machining of swept surfaces, preprint.

[32] A. Pogorui and M. Shapiro (2004), On the structure of the set of zeros of quaternionic polynomials, *Complex Variables* **49**, 379–389.

[33] R. Serôdio, E. Pereira, and J. Vitória (2001), Computing the zeros of quaternion polynomials, *Comput. Math. Applic.* **42**, 1229–1237.

[34] A. Sestini, L. Landolfi, and C. Manni (2013), On the approximation order of a space data dependent PH quintic Hermite interpolation scheme, *Comput. Aided Geom. Design* **30**, 148–158.

[35] Z. Sir and B. Jüttler (2007), C^2 Hermite interpolation by Pythagorean–hodograph space curves, *Math. Comp.* **76**, 1373–1391.

[36] N. Topuridze (2009), On roots of quaternion polynomials, *J. Math. Sci.* **160**, 843–855.

[37] D. J. Walton and D. S. Meek (1996), A Pythagorean–hodograph quintic spiral, *Comput. Aided Design* **28**, 943–950.